













Friedelin Could Moderately Modulate Human Carbonic Anhydrases: An *in Silico* Study

Toluwase Hezekiah Fatoki^{1,*}, Bolanle Christianah Faleye², Onyinyechi Ruth Nwagwe¹, Oladoja Abosede Awofisayo³, Catherine Joke Adeseko⁴, Temitope Olawale Jeje¹, Michael Eniola Ayenero⁴, Jesupemi Mercy Fatoki⁵, Olapade Samuel Akinlolu⁶, Daniel Uwaremhevo Momodu⁶, Jesufemi Samuel Enibukun⁷, Ngozi Faith Omuekwu⁸

¹ Department of Biochemistry, Federal University Oye-Ekiti, Ekiti State, Nigeria; toluwase.fatoki@fuoye.edu.ng (T.H.F.), onyinyechi.nwagwe@fuoye.edu.ng (O.R.N.), temitope.jeje@fuoye.edu.ng (T.O.J.);

² Department of Chemical Science, Joseph Ayo Babalola University, Osun State, Nigeria; bolanlefaleye77@gmail.com (B.C.F.);

³ Department of Pharmaceutical and Medicinal Chemistry, University of Uyo, Akwa-Ibom State, Nigeria; oladojaawofisayo@uniuyo.edu.ng (O.A.A.);

⁴ Department of Biochemistry, Federal University of Technology Akure, Ondo State, Nigeria; catherineadeseko@gmail.com (C.J.A.), meayenero@gmail.com (M.E.A.);

⁵ Department of Microbiology, Federal University of Technology Akure, Ondo State, Nigeria; jesupemienibukun@gmail.com (J.M.F.);

⁶ Department of Chemistry, Federal University Oye-Ekiti, Ekiti State, Nigeria; olapade.akinlolu@fuoye.edu.ng (O.S.A.), daniel.momodu@fuoye.edu.ng (D.U.M.);

⁷ College of Health Sciences, University of Ilorin, Kwara State, Nigeria; eni4suresuccess21@gmail.com (J.S.E.);

⁸ Department of Microbiology, Federal University Oye-Ekiti, Ekiti State, Nigeria; ngozi.omuekwu@gmail.com (N.F.O.);

* Correspondence: toluwase.fatoki@fuoye.edu.ng (T.H.F.);

Scopus Author ID 57211491082

Received: 14.04.2023; Accepted: 28.05.2023; Published: 4.02.2024

Abstract: Friedelin (friedelan-3-one or 3-oxofriedelane), a plant metabolite, is a pentacyclic triterpenoid with pharmacological properties that include anti-inflammatory, antioxidant, analgesic, antipyretic, antimicrobial, anticonvulsant, anti-ulcer and anti-tumor activities. This current study aims to evaluate the molecular biological targets of friedelin in humans bioinformatically. The bioinformatics methods used are target prediction, pharmacokinetic prediction, molecular docking, molecular dynamics simulation, and MMGBSA calculation. The results showed that friedelin targeted carbonic anhydrase (CA) genes in humans with about 50% probability. Friedelin has low gastrointestinal absorption, not affected by p-glycoprotein and cytochrome P450s. The phylogeny revealed that the CAs of *Vibrio cholerae* and *Streptococcus pneumoniae* are closely related to those of humans. The binding of friedelin to human CA proteins was in the order of CA I > CA II > CA IV, with different binding site amino acid residue interactions. The MMGBSA results indicate improved stability and binding energy of the complex of friedelin with carbonic anhydrase CA I from -31.190 to -34.911 kcal.mol⁻¹ at 0 ns and 100 ns, respectively. In conclusion, this study has provided the predictive potential of friedelin as a bioactive compound that could modulate the activity of various carbonic anhydrases to a moderate degree.

Keywords: friedelan-3-one; carbonic anhydrases; phylogenetics; molecular docking; molecular dynamic simulation; antimicrobial; anti-ulcer.

© 2024 by the authors. This article is an open-access article distributed under the terms and conditions of the Creative Commons Attribution (CC BY) license (<https://creativecommons.org/licenses/by/4.0/>).

1. Introduction

Friedelin (also known as friedelan-3-one or 3-oxofriedelane), is the most highly rearranged pentacyclic triterpene in plants and serves as a precursor to many other important compounds, such as saponins and sterols [1,2]. Friedelin was a compound isolated in 1892 by Friedel, and it has been found in many plants, algae, lichen, mosses, and mineral wax [3]. Friedelin is the most prominent triterpenoid in cannabis, at a concentration of 12.8 mg/kg in the root extract [4], and presents as a major constituent of *Garcinia latissimi* [5].

Luan et al. [6] have isolated friedelin from the fruit and leaf extracts of *Couroupita guianensis*. Friedelin has been identified in the stem bark, fruit peel, and pulp extracts of *Irvingia gabonensis* [7,8]. Friedelan-3-one was found as part of the constituents of *Hymenocardia acida* Tul. [9], and *Vernonia auriculifera* [10]. Friedelin and friedooleanan-3-ol were isolated from the stem bark of *Talipariti elatum* in Cuba by gas chromatography-mass spectrometry (GC-MS) method [11]. Friedelin (3-oxofriedelane) and its set of derivatives have been identified in the hexane extract of the leaves of *Maytenus robusta* [12] and hexane extracts of leaves and branches of *Tontelea micrantha* [13]. Friedelin and friedelan-3-ol were found present in *Maytenus ilicifolia* in 15 native populations in the south and mid-west regions of Brazil. [14], as well as in dichloromethane-methanol (1:1) extract of the stem bark of *Calophyllum inophyllum* [15].

Friedelin has been reported for strong anti-tumor activities and significant lipid-lowering effects [16,17]. Friedelan-3-one isolated from the ethyl acetate extract of the leaf of *Pterocarpus santalinoides* showed moderate antimicrobial activity against microbes such as *Escherichia coli*, *Helicobacter pylori*, and methicillin-resistant *Staphylococcus aureus* [18]. Friedelin showed antimycobacterial activity against three nonpathogenic species and thus served as a natural African antituberculosis agent [19]. Five friedelane triterpenes (3-friedelone, 28-hydroxy-3-friedelanone (canophyllol), 28-hydroxyfriedelan-3-one (canophyllal), 29-hydroxy-3-friedelanone, and 30-hydroxy-3-friedelanone), were found present in *Euonymus hederaceus*, a reputable medicinal plant noted for its antibiotic and anti-tumor properties [20,21]. Animal studies have shown that friedelin isolated from *Azima tetracantha* possessed significant analgesic, antipyretic, anti-inflammatory, and anti-ulcer effects [22,23], and that it possessed marked antioxidant and liver protective effects in CCl₄-induced oxidative stress on rats [24]. Also, friedelin exhibits remarkable antidiabetic activity in rat models through modulation of glucose metabolism in the liver and muscle [25].

However, the supply of friedelin from plant sources is insufficient; while chemical methods are often complex, synthetic biology and metabolic engineering have provided promising and green approaches to reconstruct microorganisms to yield natural high-value products [2,26,27]. Based on the promising pharmacological activities and presence of friedelin in many medicinal plants, identifying the key biological target enzymes or receptors or transcription factors that are responsible for these activities will facilitate the translation of friedelin to clinical development as human therapeutics. This study aims to bioinformatically evaluate the molecular biological targets of friedelin in humans to facilitate its development as therapeutic.

2. Materials and Methods

2.1. *In silico* target prediction and ADME properties.

The structure of friedelin was obtained from the PubChem Compound Database (<https://pubchem.ncbi.nlm.nih.gov/>) in canonical Simplified Molecular Input Line Entry Specification (SMILES) and Structure Data File (SDF) formats. Target prediction was done using the SwissTargetPrediction server (<http://www.swisstargetprediction.ch/>), where *Homo sapiens* was designated as the target organism [28]. *In silico* ADME (Absorption, Distribution, Metabolism, and Excretion), a prediction was carried out on the SwissADME server [29].

2.2. Phylogenetic analysis.

Targeting bacterial carbonic anhydrase (CA, EC 4.2.1.1) as an emerging mechanism for design of anti-infectives, the protein sequences of human and ten (10) bacteria (*Neisseria* spp., *Escherichia coli*, *Helicobacter pylori*, *Mycobacterium tuberculosis*, *Brucella* spp., *Streptococcus pneumoniae*, *Salmonella enterica*, *Haemophilus influenzae*, *Staphylococcus aureus*, and *Vibrio cholerae*) carbonic anhydrases were obtained from UniProt database in FASTA format, and multiple sequence alignment was done on ClustalO server (<https://www.ebi.ac.uk/Tools/msa/clustalo/>). The phylogenetic tree was obtained and visualized on iTOL server, <https://itol.embl.de/upload.cgi>; [30].

2.3. Ligand-protein docking simulations.

The molecular docking simulations were carried out using the method of Fatoki et al. [31]. Briefly, the structures of carbonic anhydrases I, II, and IV were obtained from PDB database (www.rcsb.org/pdb) in pdb format. The structure of friedelan-3one was converted from sdf format to pdb format using PyMol v2.0.7. The crystal structure of the protein targets was prepared for docking by removing all water molecules, multichain, and heteroatoms using PyMol v2.0.7. The Gasteiger partial charge was added to each ligand, and the docking parameter of each target was set using AutoDock Tools (ADT) v1.5.6 [32], and files were saved in pdbqt format. Molecular docking simulation was implemented in AutoDock Vina v1.2.3 [33,34] from the command line. The binding pose was visualized using ezLigPlot on ezCADD web server [35], the binding affinity and interacting amino acid residues were reported. The ligand efficiency (LE) was evaluated from the equation,

$$LE = \frac{-\Delta G}{HA}$$

where ΔG is the binding affinity obtained from docking, and HA is the number of heavy atoms (non-hydrogen atoms) of the ligand obtained from ADME properties [36-38].

2.4. Molecular dynamics simulations.

Molecular dynamics simulations were performed for 100 nanoseconds using Desmond, a Package of Schrödinger LLC [39-41]. The initial protein and ligand complexes stage for molecular dynamics simulation was obtained from docking studies. The protein–ligand complexes were preprocessed using Maestro's protein preparation wizard, which also included optimization and minimization of complexes. All systems were prepared by the System Builder tool. The Solvent Model with an orthorhombic box was selected as TIP3P (Transferable Intermolecular Interaction Potential 3 Points). The Optimized Potential for Liquid Simulations

(OPLS)-2005 force field was used in the simulation [42]. The models were made neutral by adding counter ions 0.15 M NaCl to mimic the physiological conditions. The NPT ensemble (Isothermal-Isobaric: moles (N), pressure (P), and temperature (T) are conserved) with 300 K temperature and 1 atm pressure was selected for complete simulation. The models were relaxed before the simulation. The trajectories were saved after every 100 ps during simulation, and post-simulation analysis of the trajectories was done to determine the root-mean-square deviation (RMSD), radius of gyration (Rg), root-mean-square fluctuation (RMSF), solvent accessibility surface area (SASA), protein-ligand interaction profile. Also, prime molecular mechanics/generalized Born surface area (MMGBSA) was calculated as follows:

$$\text{MMGBSA } \Delta G^{\text{bind}} = \Delta G^{\text{complex}} - \Delta G^{\text{protein}} - \Delta G^{\text{ligand}}$$

$$\begin{aligned} \text{MMGBSA } \Delta G^{\text{bind}} &= \Delta G^{\text{Coulomb}} + \Delta G^{\text{Covalent}} + \Delta G^{\text{Hbond}} + \Delta G^{\text{Lipo}} + \Delta G^{\text{Packing}} \\ &+ \Delta G^{\text{SolvGB}} + \Delta G^{\text{vdW}} \end{aligned}$$

where "protein*" means "protein from optimized complex"; "ligand*" means "ligand from optimized complex"; ΔG^{bind} is the total Prime energy, Hbond denote hydrogen bonding energy, Lipo is lipophilic energy, Packing represents pi-pi packing correction. SolvGB is generalized Born electrostatic solvation energy, and vdW is Van der Waals energy [41,43,44].

3. Results and Discussion

The results show that friedelin targeted carbonic anhydrase (CA) genes in humans with about 50% probability as the main molecular target (Table 1). The ADME geometry of the friedelin structure is shown in Figure 1, while the ADME properties are listed in Table 2. Friedelin (with a molecular weight of 426.72 g/mol) is poorly soluble in water, has low gastrointestinal absorption, cannot permeate the blood-brain barrier (BBB), is not affected by p-glycoprotein (P-gp), does not inhibit cytochrome P450s (CYPs), and highly lipophilic (Table 2).

The results of multiple sequence alignment showed segments of the human and bacterial CAs that are conserved over the period of evolution (Figure 2). The phylogeny revealed that the CAs of *Vibrio cholerae* and *Streptococcus pneumoniae* are closely related to those of humans (Figure 3). The order of CA proteins to which friedelin binds is CA I > CA II > CA IV, with different binding site amino acid residues interaction (Table 3). The docking pose and interaction of friedelin with human CAs are shown in Figure 4.

Friedelin and its derivatives, such as celastrol, provide potential resources for developing new drugs or dietary supplements [1,45]. The ADME properties of friedelin limit its oral route of drug administration as a systemic-acting agent. Still, it is useful in treating stomach diseases such as ulcers and topically acting agents, and intravenous administration of friedelin might not affect CYPs, which occurs during the first-pass metabolism of xenobiotics [46].

Clinical applications of various carbonic anhydrase inhibitors (CA) include the treatment of epilepsy, glaucoma, obesity, osteoporosis, mountain sickness, and ulcers [47,48]. The inhibition of the CAs is also emerging for designing anti-infectives (antifungal and antibacterial agents) with a novel mechanism of action [48,49].

In addition to carbonic anhydrases (CA II and CA IV) and cytochrome P450 19A1 obtained in this study, other molecular targets that have been reported for friedelin in the

treatment of ulcerative colitis include androgen receptor, cyclooxygenase-1, steroid 5-alpha-reductase 1, C–C chemokine receptor type 2, cannabinoid receptor 1, testis-specific androgen-binding protein, and progesterone receptor [50].

Close evolutionary relatedness of human CAs to that of CAs of *V. cholerae* and *S. pneumoniae* has the potential to design specific drugs against cholera and pneumonia infections. This study has shown that friedelin has a higher affinity for CA I, and its affinity to CA II and CA IV are almost similar, and these were evident by the binding energy and ligand efficiency obtained. The higher LE, the higher the efficiency of the drug in terms of molecular recognition per atom [37]. *In silico* study has reported the antiviral potential of friedelan-3-one with high binding energies against 2'-O-ribose methyltransferase, 3-Chymotrypsin-like protease (3CLpro), helicase, Papain-like protease (PLpro), RNA-dependent RNA polymerase, of SARS-CoV-2 [51].

Based on the results of this study, friedelin could be used to manage osteopetrosis due to a defect in human CA II and retinitis, which occurs due to a defect in human CA IV. Partial or total loss of activity of CA II due to mutation of His94 to Tyr94, His107 to Tyr107, and Gly144 to Arg144 have been linked to osteopetrosis autosomal recessive 3 (OPTB3), is a rare genetic disease characterized by abnormally dense bone, that has been implicated in cerebral calcification (marble brain disease), renal tubular acidosis, and in some cases with mental retardation (Ref.: <http://www.uniprot.org/uniprot/P00918>).

The reported functional activity of friedelin as an anticonvulsant and anti-ulcer agent matched the predicted target CAs obtained in this study [52,53]. The friedelan-3-one isolated from *Harungana madagascariensis* Lam (Hypericaceae) seeds extracts were reported for about 83% anticonvulsant activities in Albino Swiss mice induced with picrotoxin and pentylentetrazole respectively [54].

Table 1. Predicted human protein targets for friedelin compound (PubChem CID: 91472).

SNo.	TARGET			Percentage (%) Probability of Binding on Target
	Name	Gene ID	UniProt ID	
1	Carbonic anhydrase II	CA2	P00918	50
2	Carbonic anhydrase I	CA1	P00915	50
3	Carbonic anhydrase IV	CA4	P22748	50
4	Cytochrome P450 19A1	CYP19A1	P11511	20
5	Acyl coenzyme A:cholesterol acyltransferase	CES1	P23141	20
6	Carboxylesterase 2	CES2	O00748	20
7	Nuclear receptor subfamily 1 group I member 3 (by homology)	NR1I3	Q14994	20

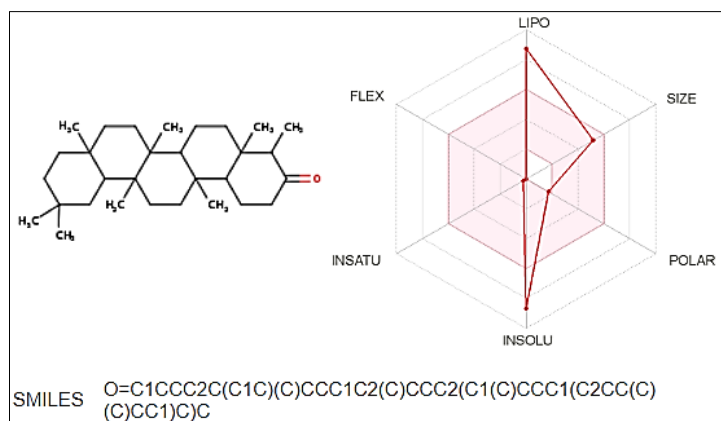


Figure 1. Structure of friedelin and its ADME geometry.

Table 2. ADME properties of friedelin in humans.

S.No	Physicochemical Properties, Water Solubility, Pharmacokinetics, Lipophilicity, Druglikeness, and Medicinal Chemistry of Friedelin	
	Properties	Value
1	Molecular weight	426.72 g/mol
2	Number of heavy atoms (HA)	31
3	Molar Refractivity	134.39
4	Topological Polar Surface Area	17.07 Å ²
5	Log S (ESOL)	-8.66
6	Solubility Class	Poorly soluble
7	Gastrointestinal absorption	Low
8	BBB permeant	No
9	P-gp substrate	No
10	CYPs inhibitor	No
11	Log Kp (skin permeation)	-1.94 cm/s
12	XLOGP3	9.80
13	Lipinski	Yes; 1 violation: MLOGP>4.15
14	Bioavailability Score	0.55
15	Synthetic accessibility	5.17

The human cytosolic CAs include CA I and CA II, while human membrane-associated CAs include CA IV, CA IX, CA XII, and CA XIV [47], and CA II can also be localized on the cell membrane. CA I and CA II are present in the mammalian red blood cells, with low expression of CA I patients with hemolytic anemia, thus serving as a marker [55,56]. CA II and CA IV could interact with a diversity of membrane-bound carriers to balance cytoplasmic pH, increase the activity of bicarbonate transport, and create a functional complex; these carriers include the sodium bicarbonate cotransporter NBC1, the chloride/bicarbonate exchanger AE1, and the sodium/hydrogen exchanger NHE1 [57-59].

CA IV is a high-activity isozyme showing pH independence in the hydration direction [60]. CA IV has been found localized to the brain, capillary bed of the eye, erythrocytes, and heart. The kidney expresses CA II, CA IV, and CA XII [47]. CA IX and CA XII are cancer-related CAs [61,62]. Thus, the CAs obtained in this study have a different function: non-cancer targets. Therefore, friedelin could be used to distinguish between CA IV and CA XII functions in the kidney.

Like friedelin, naturally produced coumarin has been identified as a very potent inhibitor of bovine CA II, and it could also inhibit a spectrum of human CAs in an unprecedented time-dependent manner [63,64]. The catalytic activity of human CA II could be dependent on the amino acid residues His 64 and His 94, as obtained in this study. The amino acids residues His64, Asn67, His94, His96, His119, Phe131, and Glu238 were found in the interaction of coumarin with human CA II [64], while Asn62, Asn67, Asn92, Val142, Leu197, Thr198, Thr199, Pro200, Leu203, and Trp208, were reported in the interaction of (C)-xylariamide A with human CA II [65]. Moreover, a recent study has predicted that tyrosol could bind to human CA II with a 100% probability [66].

In the results shown in Figure 5, the friedelin complex with carbonic anhydrase CA1 (1CZM) has RMSD of about 1.0 Å, and the protein was quite stable during the simulation time 20-100ns while the ligand RMSD was showed to be stabilized between 40-100 ns. Overall, the ligand was stable during the simulation. Also, the result showed that carbonic anhydrase CA1 has $R_g < 0.3$ Å, RMSF was significant mostly at the N-terminal and 110-120 amino acid residues, and total SASA was about 1110 Å². In Figure 6, high interaction of friedelin with carbonic anhydrase CA1 occurs on ASN61, PHE91, ALA132, ALA135, LEU198, PRO202,

and TYR204 amino acid residues and also present the profiles of friedelin during the simulation. The binding free energies of all complexes were calculated using MMGBSA at 0 ns and 100 ns. The results indicate improved stability and binding energy of the complex of friedelin with carbonic anhydrase CA1 from -31.190 to -34.911 kcal.mol⁻¹, as shown in Table 4.

tr	A0A656DW57 A0A656DW57_STREE	L	SKNGKEQSPINITGAE---DVLPE--LN--LNNQESAEQVENNGHTIEVSKFNPKNTL	112
tr	Q9KMP6 Q9KMP6_VIBCH	L	CAEGKNGSPIDVAQSV---EADLQP--FT--LNYQQGVVGLLNNNGHTLQAIVR--GNNPL	91
sp	P22748 CAH4_HUMAN	G	NCQKDRQSPINIVTTKAKVDKLLGR--FFFSGYDKKQWTVQNNNGHSVMMLE--NKA	98
sp	P00918 CAH2_HUMAN	---	GERQSPVDIDHTAKYDPSLKP--LS-VSYDQATSLRILNNGHAFNVFDDSDQKA	77
sp	P00915 CAH1_HUMAN	---	GNNQSPVDIKTSETKHDTSCLKP--IS-VSYNPATAKEIINVGHSHFVNFEDNDNRS	78
sp	P9WPJ7 MTCA1_MYCTU	---	PLMPSPKSHIAIVAC--MDARLDV--YRMLGIKEGEAHVIRNAGCVVTD-----D	66
tr	A0A033UA69 A0A033UA69_STAAU	N	LITTKTPNAKAVLLTC--MDTRLTELSTRALGFKNGDIKVVKNAGATISHPY----GS	74
tr	A0A2K4BZR1 A0A2K4BZR1_9STAP	Q	YETSKRPKDKAVLFTC--MDTRLQELATKALGFNNGDLKIVKNAGATITHPY----GS	74
tr	A0A7X2HH31 A0A7X2HH31_9RHIZ	D	LAE--KQSPETLVVAC--CDSRAAP--ETIFNAAPGEIFVLRNVANLIPPYEPDGEYHA	83
sp	P0ABE9 CYNT_ECOLI	Q	LAT--QQSPRTLFISS--SDSRLVP--ELVTQREPGLFVIRNAGNIVPSYGPPEP--GG	76
sp	O24855 CYNT_HELPY	S	LKT--KQKPHLFISS--VDSRVVP--NLITGKPGELYVICMGNVNPPTSYKESLS	77
sp	P9WPJ9 MTCA2_MYCTU	G	LAA--GQKPTAVIFGC--ADSRVAA--EIIFDQGLGDMFVVRTAGHVI---D----SA	82
tr	A0A0P7L0V4 A0A0P7L0V4_9NEIS	T	LAR--IQSPEFLYIGC--SDSRVTA--EELMGVQPGVEFVHRNVGNVNPID----MN	77
sp	P45148 CAN_HAEIN	E	LAD--HQTPHYLWIGC--SDSRVPA--EKLTNLEPGELFVHRNVANQVIHTD----FN	76
sp	P61517 CAN_ECOLI	K	LAQ--AQKPRFLWIGC--SDSRVPA--ERLTGLEPGELFVHRNVANLVIHTD----LN	76
tr	A0A379WFN2 A0A379WFN2_SALET	K	LAQ--AQKPRFLWIGC--SDSRVPA--ERLTGLEPGELFVHRNVANLVIHTD----LN	76
:				
tr	A0A656DW57 A0A656DW57_STREE	T	IGD---DVKLQKQ-----FHF	126
tr	Q9KMP6 Q9KMP6_VIBCH	Q	IDG---KTFQLKQ-----FHF	105
sp	P22748 CAH4_HUMAN	S	ISGGGLPAPYQAKQ-----LHL	116
sp	P00918 CAH2_HUMAN	V	LKGGPLDGTYYRLIQ-----FHF	95
sp	P00915 CAH1_HUMAN	V	LKGGPFSDSYRLFQ-----FHF	96
sp	P9WPJ7 MTCA1_MYCTU	V	IRSL-AISQRLLTGREIILLHHTDCGMLTFTDDDFKRAI-----QDETGRP	113
tr	A0A033UA69 A0A033UA69_STAAU	T	MRSL-LVAIYALGAEIIMGHKDCGMNLDVDSVIDTMKSRGITDDTLNIEHSGINI	133
tr	A0A2K4BZR1 A0A2K4BZR1_9STAP	T	MRSL-LIAIYALGAEIIMGHRDCGMNLDVDSVIDTMKSRGITDDTLNIEHSGINI	133
tr	A0A7X2HH31 A0A7X2HH31_9RHIZ	A	SAAL-EFAVQSLKVKHIVVMGHRGCGGKAALD-TEAP-----LSPSDFIG	129
sp	P0ABE9 CYNT_ECOLI	V	SAV-EYAVAALRVSDIVICGHSNCGAMTAIA---SCQC-----MDHMPAVS	120
sp	O24855 CYNT_HELPY	T	IASI-EYAIHVGQNLIIICGHSDCGACGVSVLIHDETT-----KAKTPYIA	124
sp	P9WPJ9 MTCA2_MYCTU	V	LGSI-EYAVTVLNVPLVVLGHDSGAVNAALAAIN-----DGTLP	123
tr	A0A0P7L0V4 A0A0P7L0V4_9NEIS	S	SVI-RYAVRYLKVKHIIIVCGHYNCGGVAAAMEQQD-----HGALN	118
sp	P45148 CAN_HAEIN	C	SVV-QYAVDVLKIEHIIICGHTNCGGIHAAMADKD-----LGLIN	117
sp	P61517 CAN_ECOLI	C	SVV-QYAVDVLVEHIIICGHYGCGGVAAVENPE-----LGLIN	117
tr	A0A379WFN2 A0A379WFN2_SALET	C	SVV-QYAVDVLVEHIIICGHSGCGGKAAVENPE-----LGLIN	117
:				
tr	A0A656DW57 A0A656DW57_STREE	V	ISVLYNYGD-ENQALKQIWDK--MPQAANTETELSQPISLDDFYPE--DKDYNYFEG	208
tr	Q9KMP6 Q9KMP6_VIBCH	V	VAVMYQVGS-ENPLLKVLTD--MPTKGN-STQLTQGIPLADWIPE--SKHYRYFNG	186
sp	P22748 CAH4_HUMAN	V	LFLVEAGTQVNEGFQPLVEALSNIKPKPEM-STTM-AESSLLDLLPKEEKLRHYFRYL	222
sp	P00918 CAH2_HUMAN	V	LGIFLKVGK-AKPGQLKVVVDLDSIKTKGK-SADP-TNFDPRGLLPE--SLDYWTYPG	195
sp	P00915 CAH1_HUMAN	V	LGLMKVGE-ANPKLQKVLDAQIKTKGK-RAPF-TNFDPSTLLPS--SLDFWTYPG	197
sp	P9WPJ7 MTCA1_MYCTU	L	RGFVFDVATGKLEIVTP-----	163
tr	A0A033UA69 A0A033UA69_STAAU	I	HGLVIDPHNGDLEVIQNGYEE--T-----K-----	189
tr	A0A2K4BZR1 A0A2K4BZR1_9STAP	V	HGLIIDPRTGELELVHDGYKN--T-----TSQN-----	192
tr	A0A7X2HH31 A0A7X2HH31_9RHIZ	L	HGAWFIDISTGELVMDHQTGD--F-----KRPEL-----	213
sp	P0ABE9 CYNT_ECOLI	L	HGWVYDIESGSIAAFDGTARQ--F-----VPLAANP-----RVCA-----	210
sp	O24855 CYNT_HELPY	I	FHWYIIEETGRINYNFESHF--F-----EPIGETI-----KQRK-----	216
sp	P9WPJ9 MTCA2_MYCTU	I	VGVTYQLDDGRAVLRDHIGN--I-----GEEV-----	207
tr	A0A0P7L0V4 A0A0P7L0V4_9NEIS	V	YGVFDIRTGLLKDLEIDFKA--I-----LSDIM-----KIYNV-----	210
sp	P45148 CAN_HAEIN	L	HGWVYDNDGFLVDQGMATS--R-----ETL-----EISYR-----	206
sp	P61517 CAN_ECOLI	I	HGWAYGIHDLRLDVTATN--R-----ETL-----EQRYR-----	206
tr	A0A379WFN2 A0A379WFN2_SALET	I	HGWAYSINDGLRLDVTATN--R-----ETL-----ENGYH-----	206
:				
tr	A0A656DW57 A0A656DW57_STREE	S	LTTTPCCTEGVNWIVFKNQET-VSKEQVEKFTQTLGF-----KNNRPIQDINGRQ	257
tr	Q9KMP6 Q9KMP6_VIBCH	S	LTTTPCSEGVNRIVLKEPAH-LSNQEEQLSVMGH-----NNRPVQPHNARL	234
sp	P22748 CAH4_HUMAN	S	LTTTPCDEKVVWTVFREPIQ-LHREQILAFSOKLYY-DKEQTVSMKDNVRLPQLGQRT	280
sp	P00918 CAH2_HUMAN	S	LTTPLLECVTWIVLKEPIS-VSSEQVLKFRKLNFNNGEPEELMVDNWRPAQPLKNRQ	254
sp	P00915 CAH1_HUMAN	S	LTHPPLYESVWTWICKESIS-VSSEQLAQFRSLLSNVGEDNAVPMQHNNRPTQLKGR	256
sp	P9WPJ7 MTCA1_MYCTU	---	-----	163
tr	A0A033UA69 A0A033UA69_STAAU	---	-----	189
tr	A0A2K4BZR1 A0A2K4BZR1_9STAP	---	-----	192
tr	A0A7X2HH31 A0A7X2HH31_9RHIZ	---	-----	213
sp	P0ABE9 CYNT_ECOLI	---	IPLRQPTAA-----	219
sp	O24855 CYNT_HELPY	---	SHENF-----	221
sp	P9WPJ9 MTCA2_MYCTU	---	-----	207
tr	A0A0P7L0V4 A0A0P7L0V4_9NEIS	---	SGSKDLSFDKAE--DK-----LDE-----E-----	229
sp	P45148 CAN_HAEIN	---	NAIARLSILDEENILKDH-----LEN-----T-----	229
sp	P61517 CAN_ECOLI	---	HGISNLKHKHANHK-----	220
tr	A0A379WFN2 A0A379WFN2_SALET	---	KGISALSLEYIPHQ-----	220

Figure 2. Multiple sequence alignment of 3 human CAs and 10 bacterial CAs.

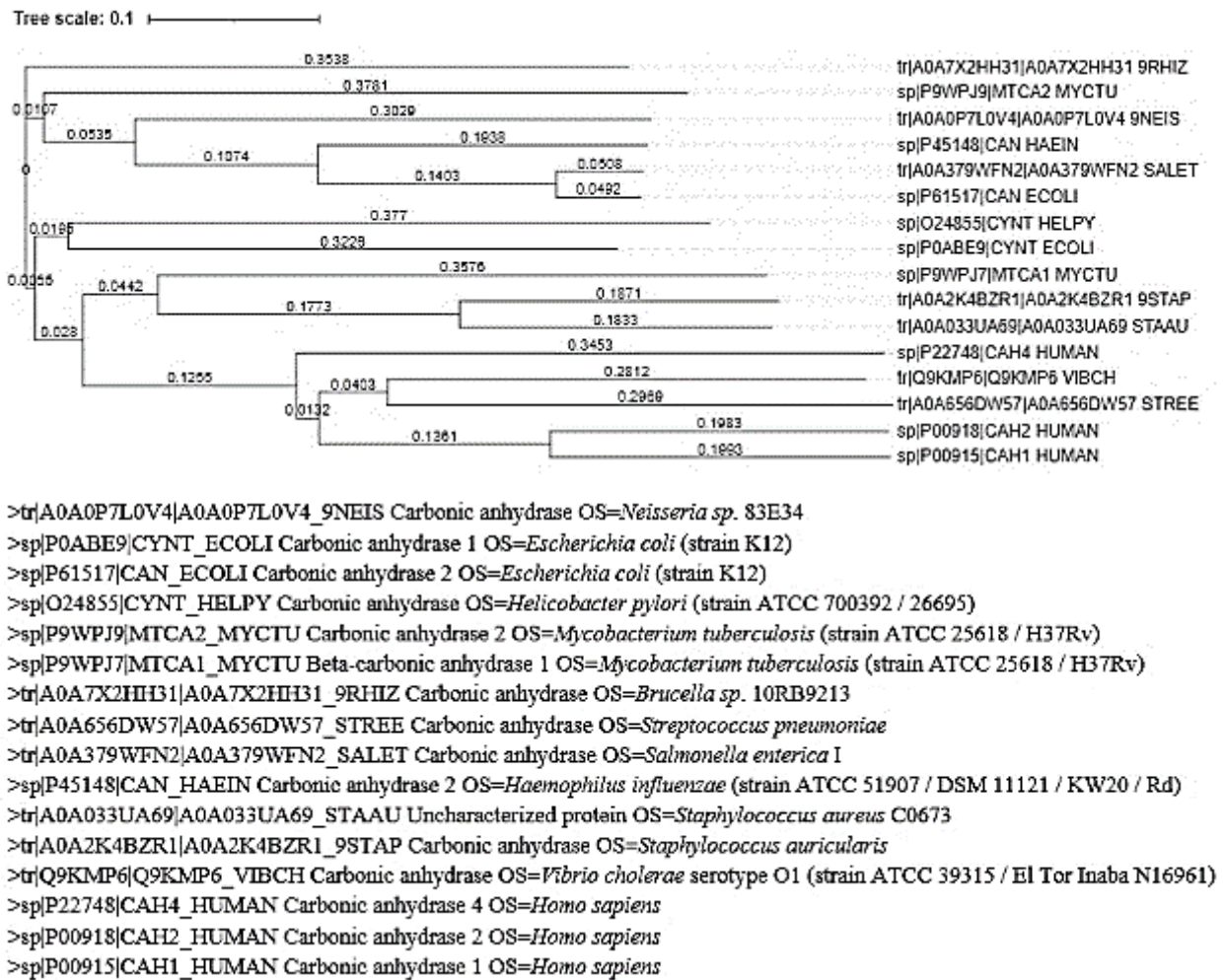


Figure 3. Phylogenetic tree of 3 human CAs and 10 bacterial CAs, and their description.

Table 3. The docking score of binding of friedelin to carbonic anhydrases.

Protein			Docking parameter	Friedelin	
Name	Gene	PDB ID		Binding Affinity (kcal.mol ⁻¹)	LE (kcal.mol ⁻¹)
Carbonic anhydrase 1	CA1	1czm	Spacing: 0.375 Npts: 126 × 126 × 126 Center: 36.650 × 14.797 × -13.116	-7.975	0.257
Carbonic anhydrase 2	CA2	1znc	Spacing: 0.375 Npts: 126 × 126 × 126 Center: 4.469 × -0.049 × 52.283	-7.441	0.240
Carbonic anhydrase 4	CA4	9ca2	Spacing: 0.375 Npts: 126 × 126 × 126 Center: -9.744 × -1.667 × 16.063	-7.310	0.236

Molecular dynamics (MD) simulation was performed to determine the variation occurring in the protein-ligand system at the atomistic level and articulate the stability of the protein-ligand complex in the dynamic environment [67]. RMSD plot indicates that most of the protein-ligand complexes were found to be stable up to 100 ns during the MD simulation. The RMSD and *Rg* are used to assess the flexibility, compactness, and conformational divergence of the protein structural ensembles [67]. RMSD scores of 1-3 Å are perfectly acceptable for small, globular proteins, while changes much greater will indicate that the protein is undergoing a large conformational change during the simulation [40].

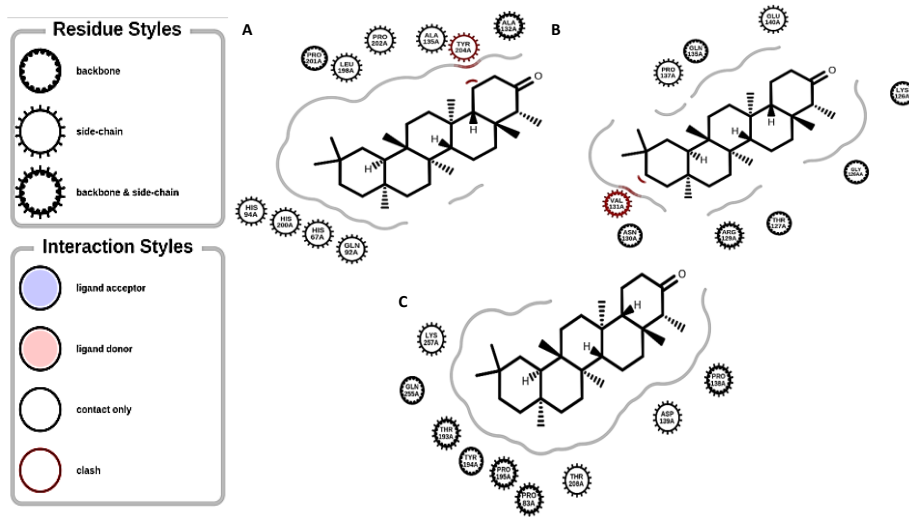


Figure 4. Docking pose and interaction of friedelin with (A) carbonic anhydrase CA1 (1CZM), (B) CA2 (1ZNC), and (C) CA4 (9CA2).

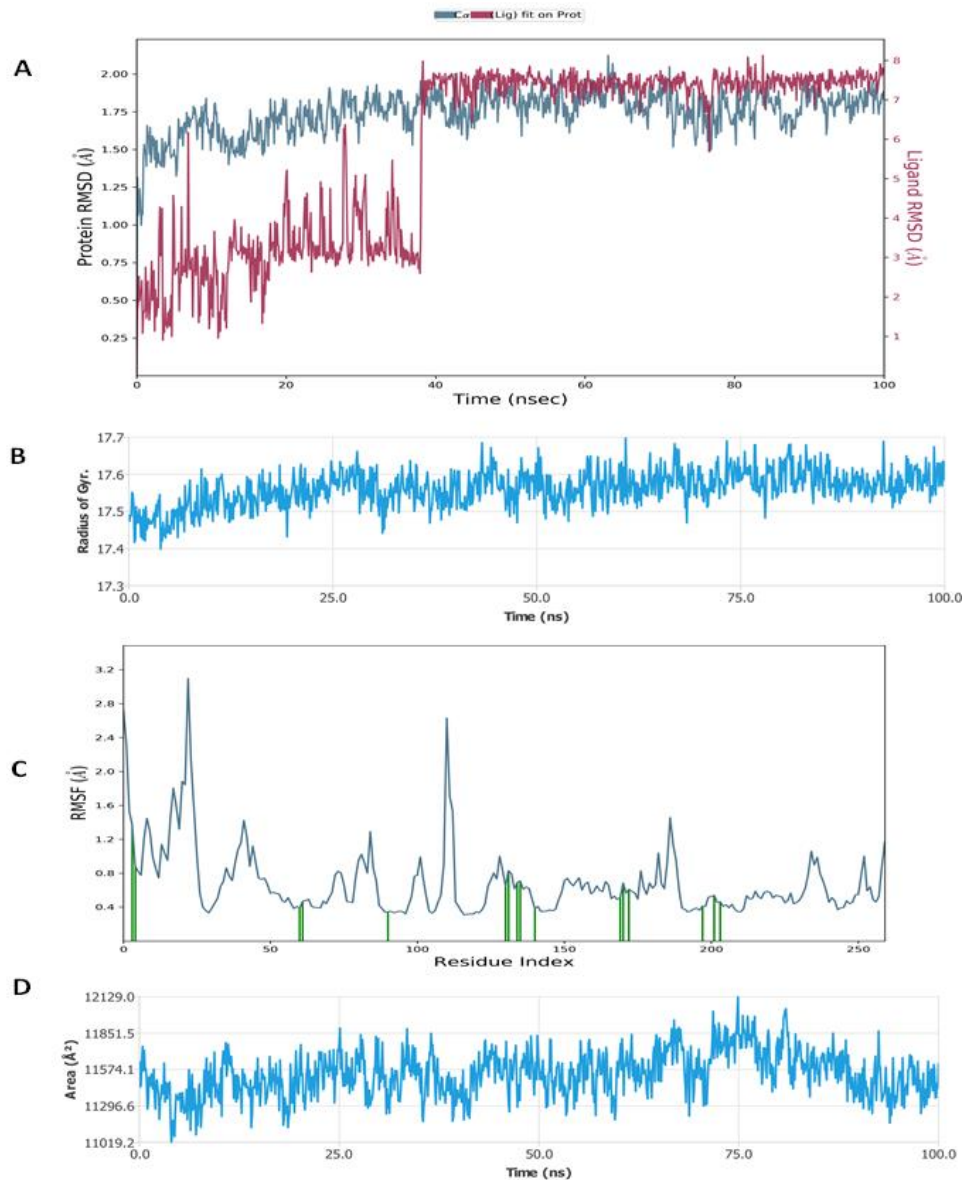


Figure 5. Molecular dynamic simulation results showing (A) RMSD of friedelin and carbonic anhydrase CA1 (1CZM); (B) Rg of carbonic anhydrase CA1 (1CZM); (C) RMSF of carbonic anhydrase CA1 (1CZM); (D) SASA of carbonic anhydrase CA1 (1CZM).

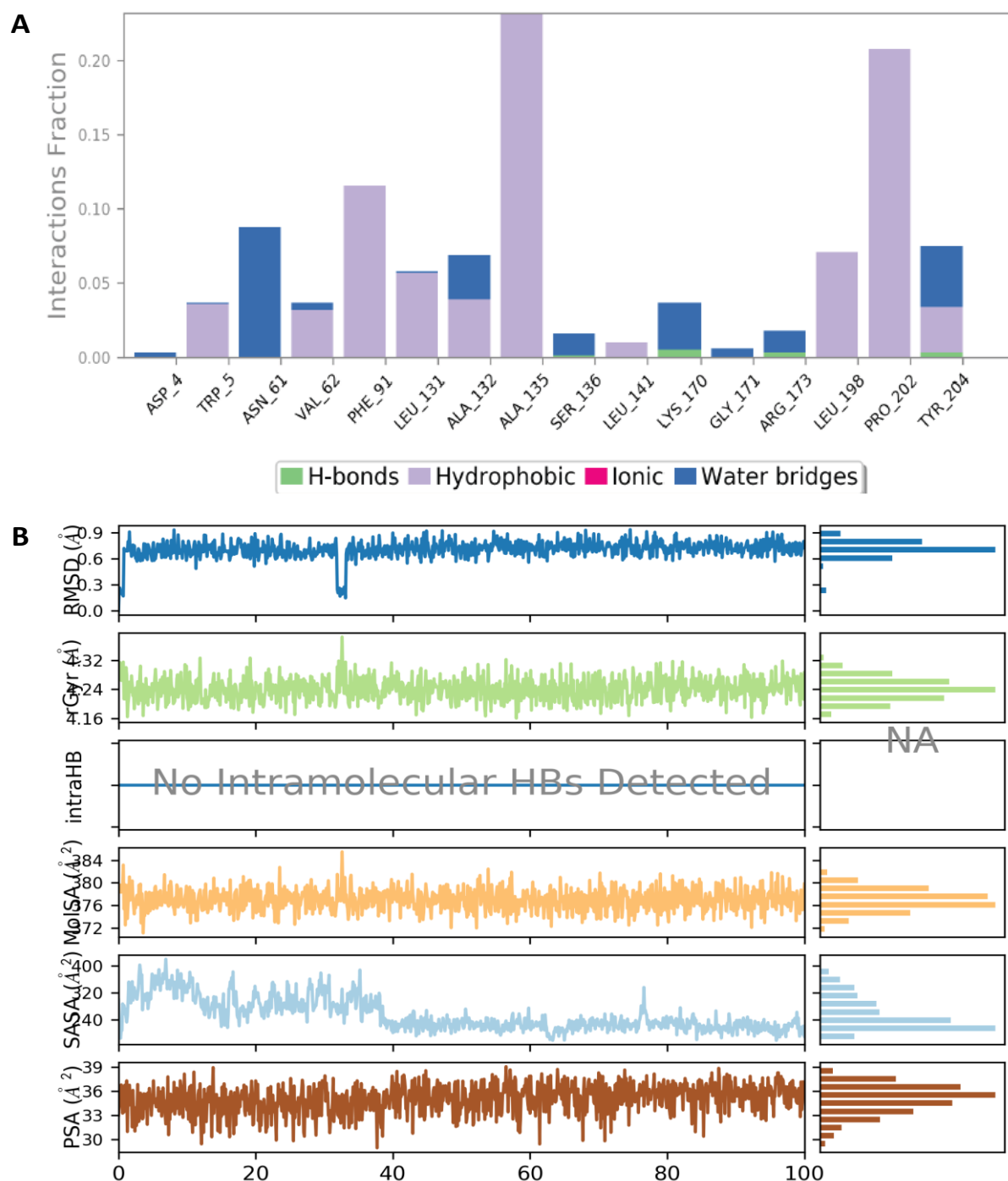


Figure 6. Molecular dynamics simulation results showing (A) Interaction profile of contact of friedelin with carbonic anhydrase CA1 (1CZM); (B) Ligand (friedelin) profile (RMSD, Rg, Intramolecular Hydrogen Bonds (intraHB), Molecular Surface Area (MolSA), SASA, and Polar Surface Area (PSA), during simulation.

Table 4. Prime MMGBSA binding energy of friedelin-carbonic anhydrase CA1 (1CZM) interaction before and after molecular dynamics simulation.

Simulation Time (ns)	MMGBSA ΔG^{bind} (kcal.mol ⁻¹)							
	Total	Coulomb	Covalent	Hbond	Lipo	Packing	Solv_GB	vdW
0	-31.190	1.041	-0.049	0	-17.674	0	17.041	-31.549
100	-34.911	-5.063	2.221	-0.028	-16.729	0	23.263	-38.575

Total: Total energy (Prime energy). Coulomb: Coulomb energy. Covalent: Covalent binding energy. vdW: Van der Waals energy. Lipo: Lipophilic energy. Solv GB: Generalized Born electrostatic solvation energy. Packing: Pi-pi packing correction.

The stability of the residues was supported by their acceptable values of the root mean square fluctuation (RMSF). RMSF is useful for characterizing local changes along the protein chain. The quantitative estimation of the binding potential of the ligand was determined using a free binding energy calculation analysis using MMGBSA. Prime MMGBSA provided various energy properties, reporting energies for the receptor, ligand, and complex structures, with energy differences related to strain and binding [43]. MM-GBSA demonstrated accurate pose prediction on a large protein-ligand complexes benchmark with non-redundant binding poses [68]. When the last frame (100 ns) of MMGBSA displayed higher binding energy as compared to the 0 ns trajectory, it indicates a better binding pose for best fitting in the protein's binding cavity [69]. The result of MMGBSA calculations shows clearly that the complexes were stable and concludes that friedelin binds efficiently to carbonic anhydrase CA1 (1CZM).

4. Conclusions

This study has provided the predictive potential of friedelin as a bioactive compound that could moderately modulate the activities of diverse sets of carbonic anhydrases and CYP P450 19A1. This pointed out that friedelin could be used to ameliorate the diseases associated with human CA I, CA II, and CA IV, as well as CAs of *Vibrio cholerae* and *Streptococcus pneumoniae*. Friedelin can potentially be developed as a new antimicrobial drug or anti-ulcer dietary supplement. Further *in vitro* and *in vivo* work will be necessary to validate this study's molecular targets and evaluate friedelin's possible host-pathogen protein-protein interactions in animal models of cholera and pneumonia diseases.

Funding

This research received no external funding.

Acknowledgments

Not applicable.

Conflicts of Interest

The authors declare no conflict of interest.

References

1. Lu, Y.; Liu, Y.; Zhou, J.; Li, D.; Gao, W. Biosynthesis, Total Synthesis, Structural Modifications, Bioactivity, and Mechanism of Action of the Quinone-methide Triterpenoid Celastrol. *Med. Res. Rev.* **2021**, *41*, 1022–1060, <https://doi.org/10.1002/med.21751>.
2. Gao, H-Y.; Zhao, H.; Hu, T-Y.; Jiang, Z-Q.; Xia, M.; Zhang, Y-F.; Lu, Y.; Liu, Y.; Yin, Y.; Chen, X-C.; Luo, Y-F.; Zhou, J-W.; Wang, J-D.; Gao, J.; Gao, W.; Huang, L-Q. Metabolic Engineering of *Saccharomyces cerevisiae* for High-Level Friedelin via Genetic Manipulation. *Front. Bioeng. Biotechnol.* **2022**, *10*, 805429, <https://doi.org/10.3389/fbioe.2022.805429>.
3. Chandler, R.F.; Hooper, S.N. Friedelin and associated triterpenoids. *Phytochemistry* **1979**, *18*, 711–724, [https://doi.org/10.1016/0031-9422\(79\)80002-3](https://doi.org/10.1016/0031-9422(79)80002-3).
4. Slatkin, D.J.; Doorenbos, N.J.; Harris, L.S.; Masoud, A.N.; Quimby, M.W.; Schiff, P.L.J. Chemical constituents of *Cannabis sativa* L. root. *J. Pharm. Sci.* **1971**, *60*, 1891–1892, <https://doi.org/10.1002/jps.2600601232>.
5. Ambarwati, N.S.S.; Azminah, A.; Ahmad, I. Molecular Docking, Physicochemical and Drug-likeness Properties of Isolated Compounds from *Garcinia latissima* Miq. on Elastase Enzyme: *In Silico* Analysis. *Pharmacogn J.* **2022**, *14*, 282–288, <http://dx.doi.org/10.5530/pj.2022.14.35>.

6. Luan, N.Q.; Thach N.P, Em N.V.M.; Trinh N.T.N.; Thao P.N.; Minh N.K.K.; Nghia N.T.; Minh P.N.; Phat N.T. Isolation and identification of triterpenoid compounds from *Couroupita guianensis* Aubl. *Can Tho Univ. J. Sci* **2023**, *15*, 91-97, <https://doi.org/10.22144/ctu.jen.2023.012>
7. Donfack, J.H.; Fosto, G.W.; Ngameni, B.; Tsofack, F.N.; Tchoukoua, A.; Ambassa, P.; Abia, W.; Tchana, A. N.; Giardina, S.; Buonocore, D.; Finzi, P.V.; Vidari, G.; Marzatico, F.; Ngadjui, B. T.; Moundipa, P.F. In vitro hepatoprotective and antioxidant activities of the crude extract and isolated compounds from *Irvingia gabonensis*. *Asian J. Tradit. Med.* **2010**, *5*, 79–88, <https://doi.org/10.1007/s10787-010-0070-4>.
8. Adeseko, C.J.; Sanni, D.M.; Salawu, S.O.; Kade, I.G.; Fatoki, T.H. HPLC-UV standard Phenolic constituents of African bush mango (*Irvingia gabonensis*) and molecular docking on polyphenol oxidases. *Journal of Applied Life Sciences International* **2019**, *22*, 1-11, <https://doi.org/10.9734/JALSI/2019/v22i130119>.
9. Igoli, O.J.; Alexander, G.I. Friedelanone and other triterpenoids from *Hymenocardia acida*. *Int. J. Phys. Sci* **2008**, *3*, 156–158.
10. Kiplimo, J.J.; Koorbanally, N.A.; Chenia, H. Triterpenoids from *Vernonia auriculifera* Hiern exhibit antimicrobial activity. *Afr. J. Pharm. Pharmacol.* **2011**, *5*, 1150-1156, <https://academicjournals.org/journal/AJPP/article-full-text-pdf/E1CC7A033259>.
11. González, J.; Cuéllar, A.; Pérez, J.; Monan, M.; Gómez, E.; (). New Chemical Compounds Isolated from the Stem Bark of *Talipariti Elatum* Sw. in Cuba. *Int. J. Adv. Res. Botany* **2018**, *4*, 14-18, <https://doi.org/10.20431/2455-4316.0401003>.
12. Sousa, G.F.; Duarte, L.P.; Alcântara, A.F.C.; *et al.*, New Triterpenes from *Maytenus robusta*: Structural Elucidation Based on NMR Experimental Data and Theoretical Calculations. *Molecules* **2012**, *17*, 13439-13456, <https://doi.org/10.3390/molecules171113439>.
13. Ferreira, F.L.; Hauck, M.S.; Duarte, L.P.; *et al.*, Zika virus activity of the leaf and branch extracts of *Tontelea micrantha* and its hexane extracts phytochemical study. *J. Braz. Chem. Soc.*, **2019**, *30*, 793-803, <https://doi.org/10.21577/0103-5053.20180210>.
14. Mossi, A.J.; Mazutti, M.; Paroul, N.; Corazza, M.L.; Dariva, C.; Cansian, R.L.; Oliveira, J.V. Chemical variation of tannins and triterpenes in Brazilian populations of *Maytenus ilicifolia* Mart. Ex Reiss. *Braz. J. Biol.* **2009**, *69*, 339-345, <https://doi.org/10.1590/s1519-69842009000200015>.
15. Islam, Q.S.; Sohrab, H.; Sharmin, S.; Hasan, C.M. Phytochemical Investigation of *Calophyllum inophyllum* L. *Dhaka Univ. J. Pharm. Sci.* **2019**, *18*, 179-182, <https://doi.org/10.3329/dujps.v18i2.43260>.
16. Lu, B.Y.; Liu, L.L.; Zhen, X.W.; Wu, X.Q.; Zhang, Y. Anti-tumor activity of triterpenoid-rich extract from bamboo shavings (*Caulis bambfusae* in Taeniam). *Afr. J. Biotechnol.* **2010**, *9*, 6430-6436, <https://www.ajol.info/index.php/ajb/article/view/92284/81737>.
17. Duraipandiyam, V.; Al-Dhabi, N.A.; Irudayaraja, S.S.; Sunil, C. Hypolipidemic activity of friedelin isolated from *Azima tetraacantha* in hyperlipidemic rats. *Rev. Bras. Farmacogn.* **2016**, *26*, 89-93, <https://doi.org/10.1016/j.bjp.2015.07.025>.
18. Odeh, I.C.; Tor-Anyiin, T.A.; Igoli, J.O.; Anyam, J.V. *In vitro* antimicrobial properties of friedelan-3-one from *Pterocarpus santalinoides* L'Herit, ex Dc. *Afri. J. Biotech* **2016**, *15*, 531- 538, <https://doi.org/10.5897/AJB2015.15091>.
19. Chinsembu, K. C. Tuberculosis and nature's pharmacy of putative antituberculosis agents. *Acta Tropica* **2016**, *153*, 46–56, <https://doi.org/10.1016/j.actatropica.2015.10.004>.
20. Sun, C.R.; Hu, H.J.; Xu, R.S.; Yang, J.H.; Wan, H.T. A new friedelane type triterpene from *Euonymus hederaceus*. *Molecules* **2009**, *14*(7), 2650–2655. <https://doi.org/10.3390/molecules14072650>
21. Hu, H.J.; Wang, K.W.; Wu, B.; Sun, C.R.; Pan, Y.J. Chemical shift assignments of two oleanane triterpenes from *Euonymus hederaceus*. *J Zhejiang Univ Sci. B*, **2005**, *6*(8), 719–721. <https://doi.org/10.1631/jzus.2005.B0719>
22. Antonisamy, P.; Duraipandiyam, V.; Ignacimuthu, S. Anti-inflammatory, analgesic and antipyretic effects of friedelin isolated from *Azima tetraacantha* Lam. in mouse and rat models. *J. Pharm. Pharmacol.* **2011**, *63*, 1070-1077, <https://doi.org/10.1111/j.2042-7158.2011.01300.x>.
23. Antonisamy, P.; Duraipandiyam V.; Arasu, M.V.; *et al.* Protective effects of friedelin isolated from *Azima tetraacantha* Lam. Against ethanol-induced gastric ulcer in rats and possible underlying mechanisms. *Eur J Pharmacol* **2015**, <https://doi.org/10.1016/j.ejphar.2015.01.015>.
24. Sunil, C.; Duraipandiyam, V.; Ignacimuthu, S.; Al-Dhabi, N.A. Antioxidant, free radical scavenging and liver protective effects of friedelin isolated from *Azima tetraacantha* Lam. Leaves. *Food Chem.* **2013**, *139*, 860–865, <https://doi.org/10.1016/j.foodchem.2012.12.041>.

25. Sunil, C.; Irudayaraj, S.S.; Duraipandiyan, V.; Alrashood, S.T.; Alharbi, S.A.; Ignacimuthu, S. Friedelin Exhibits Antidiabetic Effect in Diabetic Rats via Modulation of Glucose Metabolism in Liver and Muscle. *J. Ethnopharmacol.* **2021**, *268*, 113659, <https://doi.org/10.1016/j.jep.2020.113659>.
26. Carsanba, E.; Pintado, M.; Oliveira, C. Fermentation Strategies for Production of Pharmaceutical Terpenoids in Engineered Yeast. *Pharmaceuticals* **2021**, *14*, 295, <https://doi.org/10.3390/ph14040295>.
27. Sun, Z.-J.; Lian, J.-Z.; Zhu, L.; Jiang, Y.-Q.; Li, G.-S.; Xue, H.-L.; et al. Combined Biosynthetic Pathway Engineering and Storage Pool Expansion for High-Level Production of Ergosterol in Industrial *Saccharomyces cerevisiae*. *Front Bioeng. Biotechnol.* **2021**, *9*, 681666, <https://doi.org/10.3389/fbioe.2021.681666>.
28. Daina, A.; Michielin, O.; Zoete, V. SwissTargetPrediction: updated data and new features for efficient prediction of protein targets of small molecules. *Nucleic Acids Res* **2019**, *47*, W357–W364, <https://doi.org/10.1093/nar/gkz382>.
29. Diana, A.; Michielin, O.; Zoete, V. SwissADME: a free web tool to evaluate pharmacokinetics, druglikeness and medicinal chemistry friendliness of small molecules. *Scientific Reports* **2017**, *7*, 42717, <https://doi.org/10.1038/srep42717>.
30. Letunic, I.; Bork, P. Interactive Tree of Life (iTOL) v4: recent updates and new developments. *Nucleic Acids Res.* **2019**, *47*, W256–W259, <https://doi.org/10.1093/nar/gkz239>.
31. Fatoki, T.; Chukwuejim, S.; Ibraheem, O.; Oke, C.; Ejimadu, B.; Olaoye, I.; Oyegbenro, O.; Salami, T.; Basorun, R.; Oluwadare, O.; Salawudeen, Y. Harmine and 7,8-dihydroxyflavone synergistically suitable for amyotrophic lateral sclerosis management: An *insilico* study. *Res. Results Pharmacol.* **2022**, *8*, 49-61, <https://doi.org/10.3897/rrpharmacology.8.83332>.
32. Morris, G.M.; Huey, R.; Lindstrom, W.; Sanner, M.F.; Belew, R.K.; Goodsell, D.S.; et al. AutoDock4 and AutoDockTools4: automated docking with selective receptor flexibility. *J. Comput. Chem.* **2009**, *30*, 2785–91, <https://doi.org/10.1002/jcc.21256>.
33. Trott, O.; Olson, A.J. AutoDock Vina: improving the speed and accuracy of docking with a new scoring function, efficient optimization, and multithreading. *J. Comput. Chem.* **2010**, *31*, 455–61, <https://doi.org/10.1002/jcc.21334>.
34. Eberhardt, J.; Santos-Martins, D.; Tillack, A.F.; Forli, S. AutoDock Vina 1.2.0: New Docking Methods, Expanded Force Field, and Python Bindings. *J. Chem. Inf. Model* **2021**, <https://doi.org/10.1021/acs.jcim.1c00203>.
35. Tao, A.; Huang, Y.; Shinohara, Y.; Caylor, M.L.; Pashikanti, S.; Xu, D. ezCADD: A Rapid 2D/3D Visualization-Enabled Web Modeling Environment for Democratizing Computer-Aided Drug Design. *J. Chem. Inf. Model*, **2019**, *59*, 18–24, <https://doi.org/10.1021/acs.jcim.8b00633>.
36. Ibraheem, O.; Fatoki, T.H.; Enibukun, J.M.; Faleye, B.C.; Momodu, D.M. *In Silico* Toxicological Analyses of Selected Dumpsite Contaminants on Human Health. *Nova Biotech. et Chimica.* **2019**, *18*, 144-153, <https://doi.org/10.2478/nbec-2019-0017>.
37. Carr, R.A.E.; Congreve, M.; Murray, C.W.; Rees, D.C. Fragment-based lead discovery: leads by design. *Drug Discovery Today* **2005**, *10*, 987-992, [https://doi.org/10.1016/S1359-6446\(05\)03511-7](https://doi.org/10.1016/S1359-6446(05)03511-7).
38. Hopkins, A.L.; Groom, C.R.; Alex, A. Ligand efficiency: a useful metric for lead selection. *Drug Discov Today* **2004**, *9*, 430-1, [https://doi.org/10.1016/S1359-6446\(04\)03069-7](https://doi.org/10.1016/S1359-6446(04)03069-7).
39. Bowers, K.J.; Chow, D.E.; Xu, H.; Dror, R.O.; Eastwood, M.P.; Gregersen, B.A.; Klepeis, J.L.; Kolossvary, I.; Moraes, M.A.; Sacerdoti, F.D.; et al. Scalable algorithms for molecular dynamics simulations on commodity clusters. Proceedings of the ACM/IEEE SC2006 Conference on High-performance Networking and Computing, Tampa, FL, USA. **2006**, <https://doi.org/10.1145/1188455.1188544>.
40. Schrödinger. Schrödinger release 2018-3. Desmond molecular dynamics system, D.E. Shaw research, New York, NY, 2018. Maestro Desmond Interoperability Tools, Schrödinger, New York, NY, **2018**. Available online: <https://www.schrodinger.com/products/desmond>.
41. Balogun, T.A.; Iqbal M.N.; Saibu O.A.; Akitubosun M.O.; Lateef O.M.; Nneka U.C.; Abdullateef O.T.; Omoboyowa D.A. (Discovery of potential HER2 inhibitors from *Mangifera indica* for the treatment of HER2-Positive breast cancer: an integrated computational approach, *Journal of Biomolecular Structure and Dynamics*, **2021**, <https://doi.org/10.1080/07391102.2021.1975570>.
42. Shivakumar, D.; Williams, J.; Wu, Y.; Damm, W.; Shelley, J.; Sherman, W. (). Prediction of absolute solvation free energies using molecular dynamics free energy perturbation and the OPLS force field. *J. Chem. Theory Comput.* **2010**, *6*, 1509-1519, <https://doi.org/10.1021/ct900587b>.

43. Schrödinger. What do all the Prime MM-GBSA energy properties mean? www.schrodinger.com/kb/1875, 2019.
44. Zhang, X.; Perez-Sanchez, H.; Lightstone, F.C. A comprehensive docking and mm/gbsa rescoring study of ligand recognition upon binding Antithrombin. *Curr. Topics Med. Chem.*, **2017**, *17*, 1631-1639, <https://doi.org/10.2174/1568026616666161117112604>.
45. Zhou, J., Hu, T., Liu, Y., Tu, L., Song, Y., Lu, Y., et al. Cytochrome P450 Catalyses the 29-carboxyl Group Formation of Celastrol. *Phytochemistry* **2021**, *190*, 112868, <https://doi.org/10.1016/j.phytochem.2021.112868>.
46. Fatoki, T.H.; Awofisayo O.A.; Ibraheem O.; Oyedele A.S.; Akinlolu O.S. *In silico* Investigation of First-Pass Effect on Selected Small Molecule Excipients and Structural Dynamics of P-glycoprotein. *Bioinformatics Biol. Insight* **2020**, *14*, 1-9, <https://doi.org/10.1177/1177932220943183>.
47. Frost S.C. Physiological Functions of the Alpha Class of Carbonic Anhydrases, In: S.C. Frost and R. McKenna (eds.), *Carbonic Anhydrase: Mechanism, Regulation, Links to Disease, and Industrial Applications*, Subcellular Biochemistry 75, Springer Science, 9-30, **2014**, https://doi.org/10.1007/978-94-007-7359-2_2.
48. McKenna, R.; Supuran, C.T. Carbonic Anhydrase Inhibitors Drug Design. In: S.C. Frost and R. McKenna (eds.), *Carbonic Anhydrase: Mechanism, Regulation, Links to Disease, and Industrial Applications*, Subcellular Biochemistry 75, Springer Science, 291-324, **2014**, https://doi.org/10.1007/978-94-007-7359-2_15.
49. Supuran, C.T. Bacterial carbonic anhydrases as drug targets: towards novel antibiotics? *Front Pharmacol* **2011**, *2*, 34, <https://doi.org/10.3389/fphar.2011.00034>.
50. Shi, B.; Liu, S.; Huang A., Zhou M.; Sun, B.; Cao, H.; Shan, J.; Sun, B.; Lin, J. Revealing the Mechanism of Friedelin in the Treatment of Ulcerative Colitis Based on Network Pharmacology and Experimental Verification. Evidence-Based Compl. *Alt. Med.* **2021**, *2021*, 1-14, <https://doi.org/10.1155/2021/4451779>.
51. Fatoki, T.H.; Ibraheem, O.; Ogunyemi, I.O.; Akinmoladun, A.C.; Ugboko, H.U.; Adeseko, C.A.; Awofisayo, O.A.; Olusegun, S.J.; Enibukun, J.M. Network Analysis, Sequence and Structure Dynamics of Key Proteins of Coronavirus and Human Host, and Molecular Docking of Selected Phytochemicals of Nine Medicinal Plants. *J. Biomolecular Struct. Dynamics* **2020**, <https://doi.org/10.1080/07391102.2020.1794971>.
52. Thiry, A.; Dogne, J.M.; Supuran, C.T.; Masereel, B. Carbonic anhydrase inhibitors as anticonvulsant agents. *Curr Top Med Chem* **2007**, *7*, 855–864, <https://doi.org/10.2174/156802607780636726>.
53. Hen, N.; Bialer, M.; Yagen, B.; Aggarwal, M.; Robbins, A.H.; McKenna, R.; Scozzafava, A.; Supuran, C.T. Anticonvulsant 4-aminobenzenesulfonamide derivatives with branchedalkylamide moieties: X-ray crystallography and inhibition studies of human carbonic anhydrase isoforms I, II, VII and XIV. *J Med Chem* **2011**, *54*, 3977–3981, <https://doi.org/10.1021/jm200209n>.
54. Signe, J.K.; Aponglen, G.A.; Ajeck, J.M.; Taiwe, G.S. Anticonvulsant activities of friedelan-3-one and n-dotriacontane both isolated from *Harungana madagascariensis* Lam (Hypericaceae) seeds extracts. *J. Med. Plants Res.* **2020**, *14*, 509-517.
55. Swenson, E.R. Respiratory and renal roles of carbonic anhydrase in gas exchange and acid–base regulation. *EXS* **2000**, *90*, 281–341, https://doi.org/10.1007/978-3-0348-8446-4_15.
56. Kuo, W.H.; Yang, S.F.; Hsieh, Y.S.; Tsai, C.S., Hwang, W.L.; Chu, S.C. Differential expression of carbonic anhydrase isoenzymes in various types of anemia. *Clin Chim Acta* **2005**, *351*, 79–86, <https://doi.org/10.1016/j.cccn.2004.07.009>.
57. Sterling, D.; Alvarez, B.V.; Casey, J.R. The extracellular component of a transport metabolon: extracellular loop 4 of the human AE1 Cl⁻/HCO₃⁻ exchanger binds carbonic anhydrase IV. *J Biol Chem* **2002**, *277*, 25239–25246, <https://doi.org/10.1074/jbc.M202562200>.
58. McMurtrie, H.L.; Cleary, H.J.; Alvarez, B.V.; Loisel, F.B.; Sterling, D.; Morgan, P.E.; Johnson, D.E.; Casey, J.R. The bicarbonate transport metabolon. *J Enzyme Inhib Med Chem* **2004**, *19*, 231–236, <https://doi.org/10.1080/14756360410001704443>.
59. Yang, Z.; Alvarez, B.; Chakarova, C.; Jiang, L.; Karan, G.; Frederick, J.M., Zhao, Y.; Sauve, Y.; Zrenner, E.; Wissinger, B.; Den Hollander, A.I.; Katz, B.; Baehr, W.; Cremers, F.P.; Casey, J.R.; Bhattacharya, S.S.; Zhang, K. Mutant carbonic anhydrase 4 impairs pH regulation and causes retinal photoreceptor degeneration. *Hum Mol Genet* **2005**, *14*, 255–265, <https://doi.org/10.1093/hmg/ddi023>.
60. Baird, T.T.; Waheed, A.; Okuyama, T.; Sly, W.S.; Fierke, C.A. Catalysis and inhibition of human carbonic anhydrase IV. *Biochemistry* **1997**, *36*, 2669–2678, <https://doi.org/10.1021/bi962663s>.

61. Ivanov, S.; Liao, S.Y.; Ivanova, A.; Danilkovitch-Miagkova, A.; Tarasova, N.; Weirich, G.; Merrill, M.J.; Proescholdt, M.A.; Oldfield, E.H.; Lee, J.; Zavada, J.; Waheed, A.; Sly, W.; Lerman, M.I.; Stanbridge, E.J. Expression of hypoxia-inducible cell-surface transmembrane carbonic anhydrases in human cancer. *Am J Pathol* **2001**, *158*, 905–919, [https://doi.org/10.1016/S0002-9440\(10\)64038-2](https://doi.org/10.1016/S0002-9440(10)64038-2).
62. Pastorekova, S.; Pastorek, J. Cancer-related carbonic anhydrase isozymes and their inhibition. In: Supuran CT, Scozzafava A, Conway J (eds) Carbonic anhydrase: its inhibitors and activators. CRC Press, Boca Raton **2004**, 255–281, <https://doi.org/10.2174/138161208783877893>.
63. Vu, H.; Pham, N.B.; Quinn, R.J. Direct screening of natural product extracts using mass spectrometry. *J Biomol Screen* **2008**, *13*, 265–275, <https://doi.org/10.1177/1087057108315739>.
64. Maresca, A.; Temperini, C.; Vu, H.; Pham, N.B.; Poulsen, S-A.; Scozzafava, A.; Quinn, R.J.; Supuran, C.T. Non-zinc mediated inhibition of carbonic anhydrases: coumarins are a new class of suicide inhibitors. *J Am Chem Soc* **2009**, *131*, 3057–3062, <https://doi.org/10.1021/ja809683v>.
65. Davis, R.A.; Hofmann, A.; Osman, A.; Hall, R.A.; Muhlschlegel, F.A.; Vullo, D.; Innocenti, A.; Supuran, C.T.; Poulsen, S.A. Natural product-based phenols as novel probes for mycobacterial and fungal carbonic anhydrases. *J Med Chem* **2011**, *54*, 1682–1692, <https://doi.org/10.1021/jm1013242>.
66. Fatoki, T.H.; Akintayo, C.O.; Ibraheem, O. Bioinformatics Exploration of Olive Oil: Molecular Targets and Properties of Major Bioactive Constituents. *Oilseeds and fats, Crops and Lipids* **2021**, *28*, 1-8, <https://doi.org/10.1051/ocl/2021024>.
67. Fatoki, T.H.; Balogun, C.T.; Oluwadare, O.T.; Famusiwa, C.D.; Oyebiyi, O.R.; Ejimadu, B.A.; Lawal, O.E.; Amosun, B.E.; Adeyeye, T.O.; Falode, J.A. *In Silico* Evaluation of Nutri-Pharmacological Potentials of Phytochemicals in Sorghum (*Sorghum bicolor*) Grains. *J. Food Bioact* **2023**, *23*. <https://doi.org/10.31665/JFB.2023.18354>.
68. Forouzesh, N.; Mishra, N. An Effective MM/GBSA Protocol for Absolute Binding Free Energy Calculations: A Case Study on SARS-CoV-2 Spike Protein and the Human ACE2 Receptor. *Molecules* **2021**, *26*, 2383, <https://doi.org/10.3390/molecules26082383>.
69. Jawarkar, R.D.; Sharma, P.; Jain, N.; Gandhi, A.; Mukerjee, N.; Al-Mutairi, A.A.; Zaki, M.E.A.; Al-Hussain, S.A.; Samad, A.; Masand, V.H.; et al. QSAR, Molecular Docking, MD Simulation and MMGBSA Calculations Approaches to Recognize Concealed Pharmacophoric Features Requisite for the Optimization of ALK Tyrosine Kinase Inhibitors as Anticancer Leads. *Molecules* **2022**, *27*, 4951, <https://doi.org/10.3390/molecules27154951>.